

Preliminary Validation of Fluid-Structure Interaction Modeling for Hypersonic Deployable Re-Entry Systems

P. Pasolini^{1,2}, R. Savino¹, F. Franco¹, S. De Rosa¹

Abstract: The aim of the present work is to provide a first attempt to set an aero-thermo-elastic methodology for deployable atmospheric re-entry decelerators operating at high Mach number and high dynamic pressure. Because of the severity of re-entry conditions such as high temperatures, high pressures and high velocities, the behavior of their flexible structures is a hard target to assess. In this paper a partitioned Fluid Structure Interaction (FSI) approach based on the integration of different commercial software (STAR-CCM+ and ABAQUS) is presented. In order to validate the specific codes and the overall strategy for structural and fluid dynamics analyses of flexible structures, different test cases are considered, including numerical and experimental literature results related to the problem under investigation. The paper shows that a good description of the physical behavior is possible with the proposed FSI partitioned approach. The model is preliminarily applied to investigate structural, fluid dynamic and aero-thermal behavior of a flexible deployable umbrella-like configuration along a typical suborbital re-entry trajectory based on sounding rocket.

Keywords: Aero-thermo-elasticity, Aero-thermal interaction, HDAD, Atmospheric re-entry

1 Introduction

The idea to build structures with deployable Thermal Protection System (TPS) for atmospheric re-entry goes back to the 1960s. Only recently, interest in these types of structures have received a strong thrust because several space missions, requiring entry in different planets atmospheres, including Earth, Mars, Titan, and Neptune [Smith, Tanner, Mahzari, Clark, Braun, and Cheatwood (2010)].

A structure, in which the TPS can be easily accommodated in launch vehicles in

¹ Department of Industrial Engineering (DII), University of Naples "Federico II", Via Claudio 21, 80125 Napoli, Italy.

² Corresponding author: Tel.: +39 0817683576. E-mail addresses: pietro.pasolini@unina.it

a folded configuration, and deployed only during re-entry phase, offers the advantage to increase the mass/volume ratio at launch, thereby providing easy payload accommodation in the launcher fairing. When deployed, the ballistic coefficient is relatively low, implying a large deceleration in the upper rarefied region of the atmosphere, with consequent reduction of the thermal and dynamic loads. The above mentioned ballistic coefficient is defined by the ratio between mass and the product of exposed surface times the drag coefficient.

Recent studies have been focused on Hypersonic Inflatable Aerodynamic Decelerator (HIAD) technology [Beck, Arnold, White, Fan, Stackpoole, Agrawal, and Coughlin (2011); Sheta, Venugopalan, Tan, Liever, and Habchi (2010); Cassell, Swanson, Keith Johnson, Hughes, and Cheatwood (2011)]. One example is the Inflatable Re-entry and Descent Technology (IRDT) [Wilde and Walther (2001)]. The most advanced program, including experimental flight test and aero-elastic assessments, is the Inflatable Re-entry Vehicle Experiment (IRVE) [Harper and Braun (2014); Hughes, Dillman, Starr, Stephan, Lindell, Player, and Cheatwood (2005); Litton, Bose, Cheatwood, Hughes, Wright, Lindell, Derry, and Olds (2011); Hughes, Cheatwood, Dillman, Wright, Del Corso, and Calomino (2011); Wang, Yang, Liu, Wang, Mignolet, and Bartels (2010); Kramer, Cirak and Pantano (2013); Goldman and Dowell (2015); Goldman, Dowell and Scott (2015); Goldman, Scott and Dowell (2014)]. Beside those, only few concepts for mechanically deployable atmospheric re-entry systems exist. One of the first concepts was a deployable capsule, developed by Akin (1990), using an umbrella-like heat shield, made of silicon fabrics, called *Parashield*.

The University of Naples “Federico II” is currently working in cooperation with other small and medium enterprises, on the development of a Hypersonic Deployable Aerodynamic Decelerator (HDAD) [Iacovazzo, Carandente, Savino and Zuppari (2015); Carandente and Savino (2014); Carandente, Zuppari and Savino (2014); Carandente, Savino, Iacovazzo and Bozza (2013); Carandente, Elia and Savino (2013); Savino and Carandente (2012)]. This research program, coordinated by the Italian and European Space Agencies, has the purpose to demonstrate the possibility to develop, in the near future, a low-cost deployable re-entry capsule to enable future space missions, including payloads return on Earth from the ISS and/or recoverable scientific experiments in Low Earth Orbit (LEO) [Carandente, Savino, D’Oriano and Fortezza (2014); Bassano, Savino, Lo Forti, Ferrarotti, Richiello, Russo, Aurigemma, Punzo, and Dell’Aversana (2011); Savino, Aurigemma, Carandente, Dell’Aversana, Gramiccia, Longo, Marraffa, and Punzo (2013)].

The characterization of the Aero-Thermo-Elastic (ATE) behavior of a flexible structure during atmospheric re-entry is obviously a Fluid-Structure-Interaction (FSI)

problem. The deflection of the flexible TPS subjected to aerodynamic and thermal loads influence the flow field, modifying in turn thermal and aerodynamic behavior. If this loop of influences results in an energy extraction from the flow stream, the structure may experience flutter, resulting in a self-oscillation of the structure, and in eventual failure.

The purpose of the present work is to set up and validate a computational methodology by proper integration of commercial codes in order to assess ATE phenomena in the pre-design study phase of a HDAD. The article is organized as follows. In Section 2 a partitioned FSI approach using commercial codes, ABAQUS for the structural analysis and Cd-Adapco STAR-CCM+ for the fluid dynamic analysis, is introduced and described. A brief description of the capsule configuration is also presented in the aforementioned section. The approach validation is proposed in Section 3, where two different test cases are considered for the thermal-structural interaction and for the aero-thermal interaction. The model is preliminarily applied to investigate the aero-thermal behavior of a flexible deployable umbrella-like configuration along a typical suborbital reentry trajectory in Section 4. Main results and conclusions are summarized in Section 5.

2 FSI Modeling approach

As mentioned in the introduction, analysis of re-entry conditions for non-lifting capsules with deployable TPS includes aero-thermo-elastic studies to predict the dynamic behavior of the flexible heat shield. The conditions that the capsule experiences during re-entry, in particular high dynamic pressure, high temperatures and high heat fluxes with consequent large deformation of the flexible structures requires an in depth analysis of the interaction between the fluid and structure. Figure 1 shows the accuracy level required from each subject of the hypersonic Aerothermoelasticity of flexible structures.

Computational Aero-Thermo-Elasticity (CATE) generally refers to coupling high-level computational fluid dynamic (CFD) solvers with high-level structural dynamic solvers (generally using FEA approach). Mc Namara and Friedman (2007), (2011), and Culler and McNamara (2010) have studied a CATE methodology incorporating heat transfer between fluid and structure using CFD-based aerodynamic heating computations.

For this type of analysis, the aerodynamic heating conditions were obtained from the CFD solver, and have been exchanged to the FEM solver that computes the thermal deflections. In his studies, Mc Namara has highlighted two categories of fluid-structural coupling namely, monolithic and partitioned. For the monolithic approach, the governing equations of the fluid and structure are combined into a

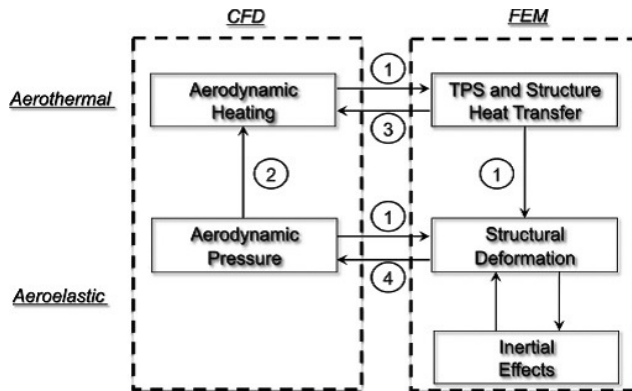


Figure 2: Basic structure of the aero-thermo-elastic problem when solved using coupled CFD and CTSD solvers [Mc Namara and Friedmann (2007)]

In this work, we have selected as a reference configuration the capsule with a flexible TPS in umbrella-like configuration presented by Iacovazzo, Carandente, Savino and Zuppari (2015); such configuration is presented in Figure 3. The relevant flight characteristics have been evaluated by Iacovazzo, Carandente, Savino and Zuppari (2015) for this deployable capsule along a typical suborbital re-entry trajectory based on sounding rocket launch. In particular, two flight conditions of the trajectory computed in aforementioned work have been considered, corresponding to the maximum heat flux and the maximum stagnation point pressure (Table 1).

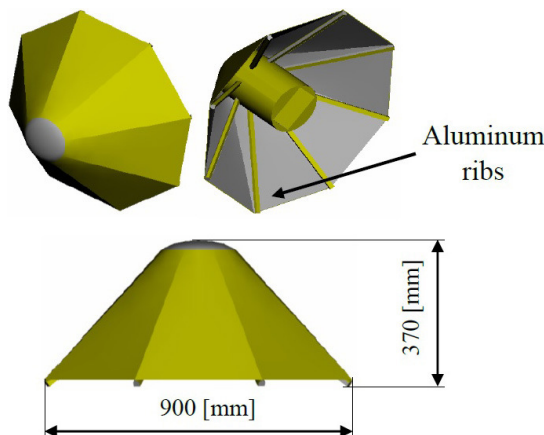


Figure 3: Schematic configuration for a re-entry demonstrator to be testes on board REXUS rocket (half cone angle 45°) [Iacovazzo, Carandente, Savino and Zuppari (2015)]

Table 1: Flight conditions at maximum heat flux and max stagnation pressure evaluated by Iacovazzo, Carandente, Savino and Zuppardi (2015)

	Altitude (Km)	Velocity (m/s)	Mach
Max Heat Flux	47.5	840	2.5
Max stagnation point pressure	40	575	1.7

Suitable test cases have been selected to perform preliminary structural, fluid dynamic and aero-thermo-dynamic analyses using the commercial software *ABAQUS* for the structural domain and *Cd-Adapco STAR CCM+* for the fluid domain.

3 Model Validation

As highlighted by Bisplinghoff and Dugundji (1958), in order to discuss the ATE problem, it is useful to extend the Collar’s triangle to a rectangle (Figure 4). In general, there are various degrees of coupling among all the rectangle elements. For example, the aero-thermo-elastic coupling is conceivable if the aero-thermal characteristic time (given by the ratio between the square of the characteristic length and the thermal diffusivity of the material) is comparable to the aero-elastic characteristic time (given by the ratio between one to natural frequency of the structure).

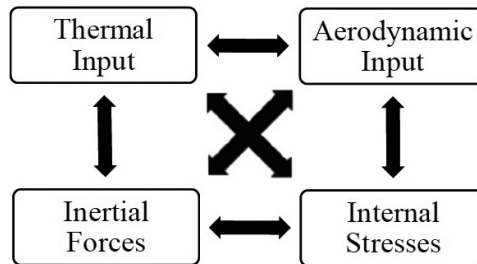


Figure 4: Aero-thermo-elastic rectangle [Bisplinghoff and Dugundji (1958)]

In order to validate a complete methodology for the coupling between all elements of the rectangle proposed by Bisplinghoff, for this preliminary work, it has been chosen to uncouple the ATE problem in two sub-coupling interaction problems with the thermal influence at center: 1) The Thermo-Structural Interaction; 2) The Aero-Thermal Interaction. Two benchmark experiments available in literature have been selected to compare the results of the present work.

3.1 Thermo-Structural Interaction

Thermo-Structural coupling using the ABAQUS code has been investigated referring to the work of Gossard, Seide and Roberts (1952). In this work, an approximate method for calculating the deflection of flat plates subjected to thermal buckling is outlined. Experimental tests on an initially imperfect plate subjected to a “tentlike” temperature distribution, for a range of differential temperatures (T_0), have also been conducted to validate theory presented by Gossard (Figure 5).

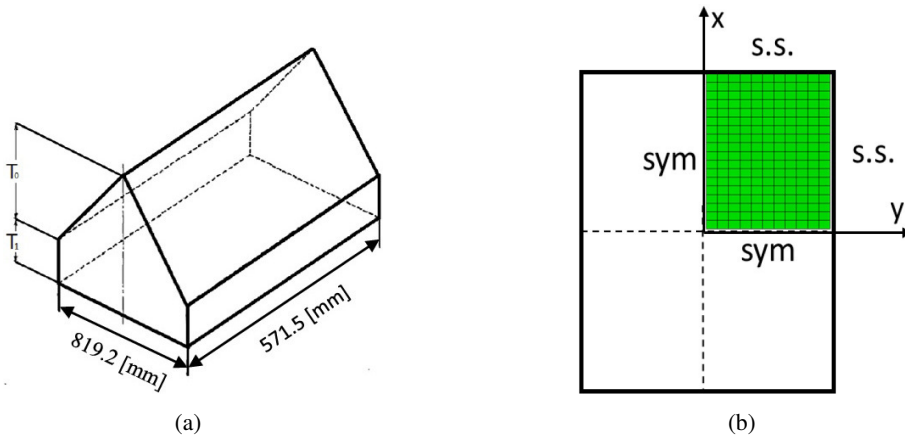


Figure 5: Panel dimensions and tentlike temperature distribution (a) and Finite Element Model with Boundary Conditions (b)

A Finite Element analysis has been developed using *ABAQUS v6.13*. Only a quarter of the panel has been modeled (Figure 5) due to symmetry. The experimental boundary conditions have been approximated as simply supported for this analysis. The material selected for the plate is an aluminum-alloy 7075-T6 with a Young modulus of 70 (GPa) and Poisson’s ratio of 0.33. The plate length and width are 819.2 (mm) and 571.5 (mm), respectively, the thickness is 6.4 (mm) and the coefficient of thermal expansion is $0.229 \cdot 10^{-4}$ ($1/^\circ\text{K}$). The plate was initially imperfect and had a center deflection of 1.14 (mm). Coupled temperature-displacement elements (S4RT) from *ABAQUS v6.13* elements library and a steady state Coupled Temperature-Displacement step have been selected, in order to assess the steady state thermo-elastic behavior of the plate.

In order to validate the ABAQUS thermo-structural analysis of plates with initial deflection, it has been chosen to compare experimental results and theoretical results obtained by Gossard, with the results obtained by the simulation presented in this work, at different values of the differential temperature T_0 (Figure 6).

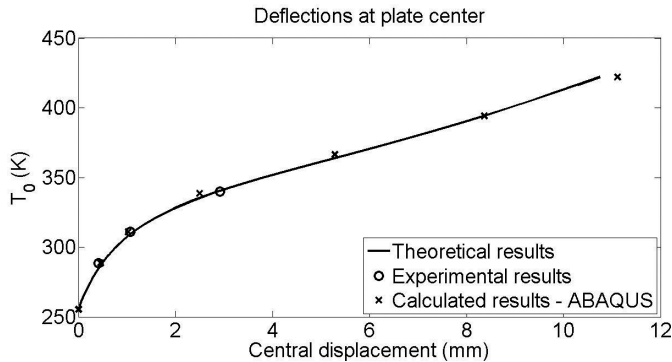


Figure 6: Comparison of plate center deflections

For the worst case of a differential temperature of 339 (K), a comparison between experimental and numerical central lines shape is presented (Figure 7).

3.2 Aero-Thermal Interaction

The Aero-Thermal Interaction has been investigated considering the work carried out at NASA Langley Research center [Del Corso, Bruce, Liles, and Hughes (2011); Glass and Hunt (1988); Hughes, Ware, Del Corso, and Lugo (2009); Deveikis and Hunt (1973); and Del Corso, Bruce, Liles and Hughes (2011)]. The aim of this work is to test several candidate materials for the TPS of the IRVE-3 experiment program for the severe thermal conditions experienced by the flexible TPS along a planetary entry trajectory.

The experimental tests have been conducted in the 8' Foot High Temperature combustion heated, hypersonic blowdown wind tunnel. The duration of the test is approximately 90 sec. A dual wedge sled was mounted in the wind gallery so that two test conditions could be run simultaneously (Figure 8).

The low-pressure conditions presented by Hughes, Ware, Del Corso, and Lugo (2009) at a sled angle of 5° have been selected (Table 2). A comparison between CFD results of the NASA's work conducted with Vulcan v6.0.1 CFD code, and CFD results conducted with *Cd-Adapco STAR-CCM+ v10.02* CFD code is summarized in Table 3.

Aero-thermal coupling has been simulated using two commercial codes, ABAQUS for the material thermal distribution, and STAR-CCM+ to solve flow motion equations and aerodynamic heating conditions. For the structural model an uncoupled heat transfer implicit scheme has been used, in which the temperature field is calculated without considering the stress/deformation study. Diffusive heat transfer

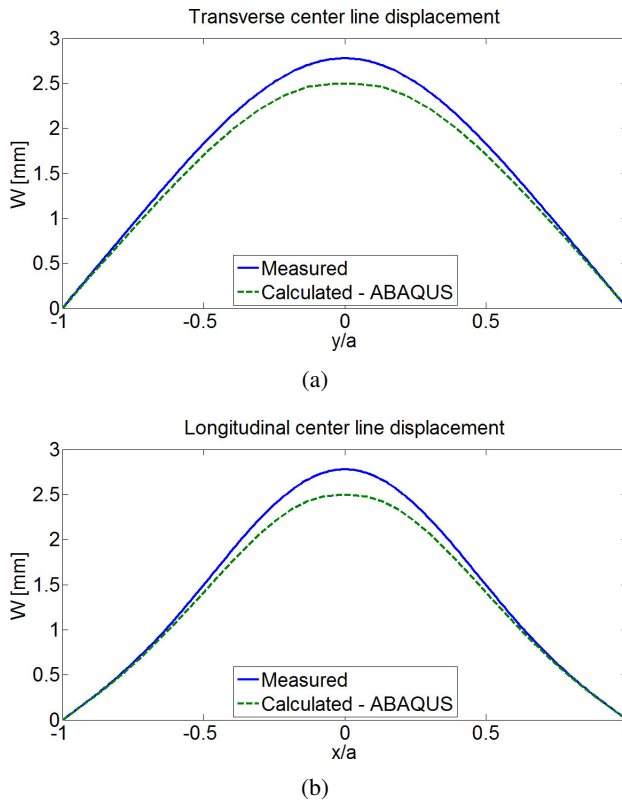


Figure 7: Comparison between transverse center line (a) and longitudinal center line (b) displacements.

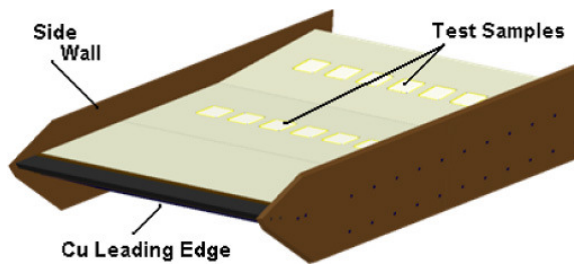


Figure 8: Sketch of the test sled [Hughes, Ware, Del Corso, and Lugo (2009)].

elements (DC3D8), have been selected from ABAQUS elements library to simulate the thermal conduction inside the texture. The flow field is turbulent and the numerical simulations have been performed with a K-Epsilon 3D, time implicit

Table 2: Definition of low-pressure tunnel conditions [Hughes et al. (2009)]

<i>Low-pressure test conditions</i>	
Composition – Mole fractions	N2 = 0.7154, O2 = 0.0237, CO2 = 0.0841, H2O = 0.1682, Ar = 0.0086
Flow Conditions	<ul style="list-style-type: none"> • Mach 7 • 813 (Pa) • 206 (K) • 2039 (m/s)

Table 3: CFD results comparison

Sample	<i>Vulcan</i>		<i>STAR-CCM+</i>		
	Sled AoA	HFL (W/cm²)	Pressure (Pa)	HFL (W/cm²)	Pressure (Pa)
10	5	11	3740	11,2	3776
5	5	5,9	1860	6,1	1848

numerical scheme. The *SIMULIA Co-Simulation Engine* solver has been used to exchange data between the two model interfaces. An implicit staggered algorithm with a time step of 0.5 seconds has been used to interchange heat transfer coefficients and temperature values between codes. As benchmark sample, we selected the layup 6 (Figure 9) placed in a forward location and the low-pressure flow condition due to the good nominal results obtained by experimental tests. The top surface of the layup 6 structural model has been coupled with the relative wall of the CFD domain according to the dimensions reported by Del Corso, Bruce, Liles and Hughes (2011); only a section of the wind tunnel has been modeled (Figure 10). The layup 6 is a Coupon TPS made of four layers. The Refrasil C1554-48 outer fabric layer is exposed directly to the Mach 7 flow in the 8’HTT. The Pyrogel 6650 insulator fabric is used to prevent excessive heating through the thickness. The Kapton fabric is intended to act as a gas barrier between the aero-shell bladder and the aero-shell TPS. All layers material properties are summarized in Table 4. As evaluated by Del Corso, Bruce, Liles, and Hughes (2011), a contact resistance of 18 (m²K/W) has been introduced to simulate the gap among texture layers.

A comparison between experimental results, aero-thermal interaction simulation methodology presented in this work, and numerical simulation results presented by Hughes, Ware, Del Corso, and Lugo (2009) is depicted in Figure 11. It should be noted that there is good agreement between the experimental test and the aero-

Table 4: Layup 6 material properties [Hughes, Ware, Del Corso, and Lugo (2009)]

Material	Layer Type	Thickness (mm)	Density (Kg/m ³)	Conductivity (W/m·K)	Specific Heat (J/Kg·K)	Emissivity
Refrasil C1554-48	Outer	0.66	924	0.865	1172	0.7
Pyrogel 6650	Insulator	6.35	110	0.01 at 0°C 0.02 at 130°C 0.03 at 480°C	1046	-
Kapton	Barrier	0.03	1468	0.12	1022	-

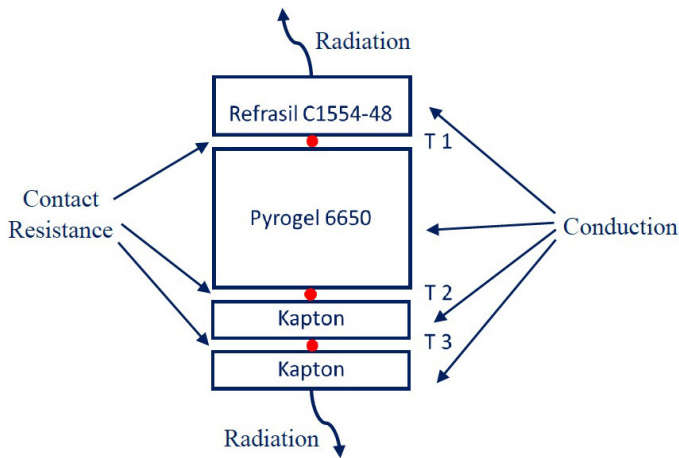


Figure 9: TPS coupon layup 6 and thermocouple locations

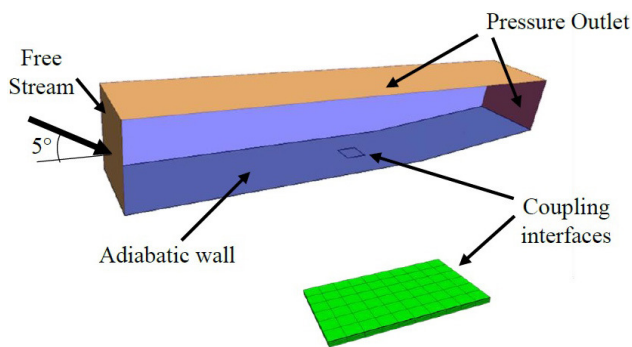


Figure 10: CFD and FEM coupling models

thermal interaction simulation. The simulation results report an average value between top and bottom node temperatures of each couple of layers. As highlighted

above, same material properties and flow conditions of the numerical simulations carried out at NASA LaRC have been used for the CFD-FEM coupling approach presented in this work.

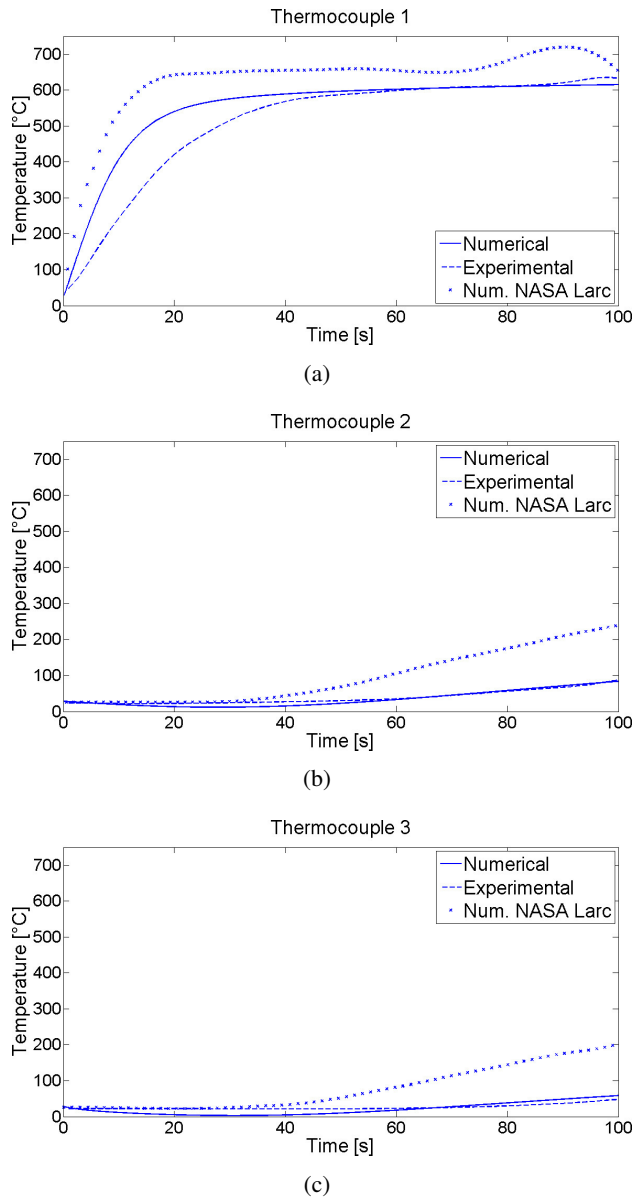


Figure 11: Comparison between experimental and numerical results

4 Preliminary uncoupled ATE analysis of deployable re-entry capsule

4.1 Fluid Dynamic Model

For the configuration considered by Iacovazzo, Carandente, Savino and Zuppari (2015) (Figure 3), and the flight conditions reported in Table 1, fluid dynamic numerical simulations have been carried out with the *Cd-Adapco STAR-CCM+* software. Due to the re-entry conditions selected, the flow field around the capsule is considered to be laminar, and the solver computes the steady three-dimensional flow field with a time implicit numerical scheme. The field equations including mass, momentum and energy conservation are solved simultaneously. A radiation model, which allows simulation of radiative heat transfer towards the ambient has been used. The radiative model takes into account the emissivity of the fabric (0.443) and of the aluminum (0.1) and an ambient temperature of 270 (K) is considered to simulate radiative heat transfer between the capsule and the surrounding ambient. A constant wall static temperature of 270 (K) has been considered to evaluate cold wall heat fluxes.

Only a quarter of the volume has been meshed and modeled due to symmetry conditions. Referring to Figure 12, free stream conditions are imposed at the domain boundary labeled as 1, no-slip conditions for the velocity and radiative equilibrium at the capsule wall (labeled as 2), pressure outlet along downstream and side surfaces (labeled as 3).

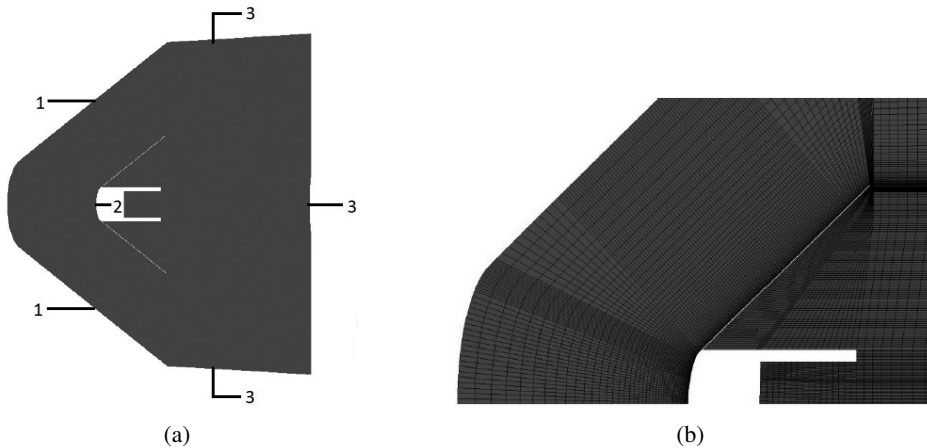


Figure 12: Computing mesh for CFD analyses

Both conditions reported in Table 1 have been simulated. For the first condition, the Mach number is 2.5 at an altitude of 47 (Km). Relative CFD results, which include

Table 5: CFD results

	H (Km)	M	\dot{q}_0 (kW/m ²)	p ₀ (kPa)
Max Heat Flux condition	47	2.5	6.7	0.95
Max stagnation point pressure condition	40	1.7	2.4	1.15

Mach number, pressure, and surface boundary heat flux, are summarized in Figure 13. Since radiative heat fluxes are not so relevant compared to the convective heat fluxes, because of the cold wall boundary condition imposed in the simulation, only convective heat flux is depicted.

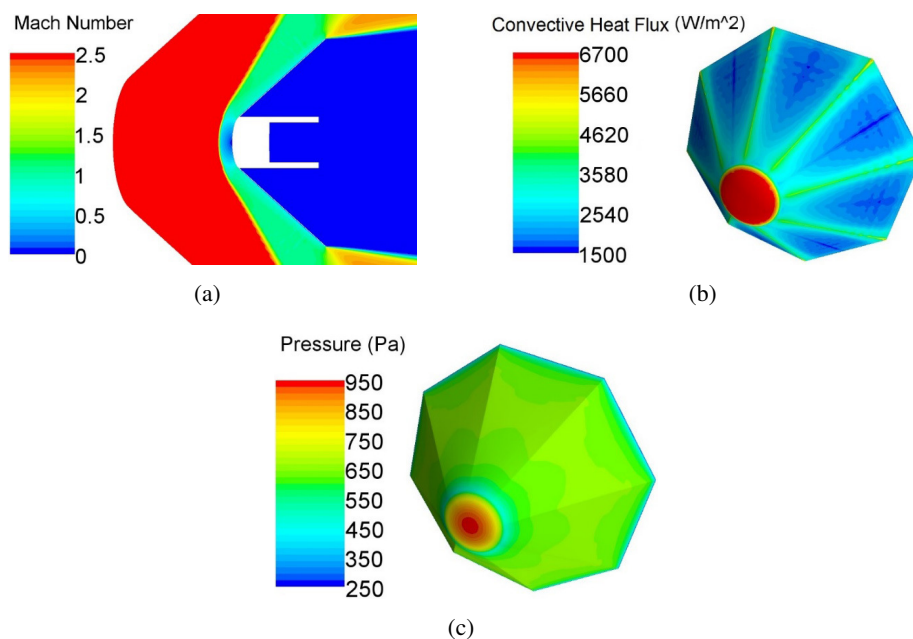


Figure 13: Maximum heat flux condition CFD Results

For the case corresponding to max stagnation point pressure condition along the entry trajectory illustrated in Table 1, main results are shown in Figure 14. Values of heat flux and stagnation point pressure, computed with the above mentioned conditions, are summarized in Table 5.

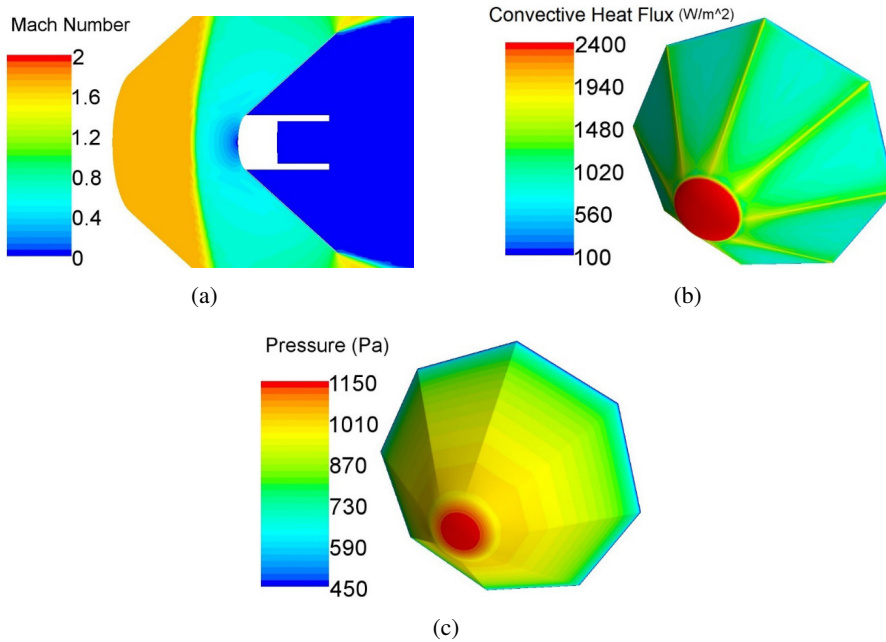


Figure 14: Maximum stagnation point pressure condition CFD results

4.2 Structural model

The structural problem has been addressed with *ABAQUS v6.13*. Since a geometrically nonlinear behavior is expected for the load application case on the thin flexible TPS of the capsule, the Newton's method with the (NLGEOM) large-displacement formulation has been used. For the capsule geometry, we selected the capsule configuration presented by Iacovazzo, Carandente, Savino and Zuppari (2015), corresponding to an octahedral shape held tensioned by 8 cylindrical ribs with a tube section of 1 (mm) thickness. A CAD model of this configuration is shown in Figure 3.

The materials chosen for the simulation are respectively Nextel BF-20 for the flexible TPS and aluminum 7075-T6 for the central body and for the ribs (see table 6 for material properties). A single layer of Nextel of 0.5 (mm) of thickness has been used for the structural simulation.

A brief description of the model and elements used for the simulation is shown in Figure 15. For the sake of simplicity, only half capsule has been modeled and symmetry boundary conditions have been applied at symmetry plane location.

According to the results obtained by CFD simulation (Table 5), a constant value of the maximum pressure at stagnation point of 1.15 (kPa) has been applied on the

Table 6: Structural model material properties

Material	Thickness (mm)	Density (Kg/m ³)	Young modulus (GPa)	Poisson's ratio
Nextel BF-20	0.5	2700	150	0.33
Aluminum 7075-T6	-	2700	70	0.33

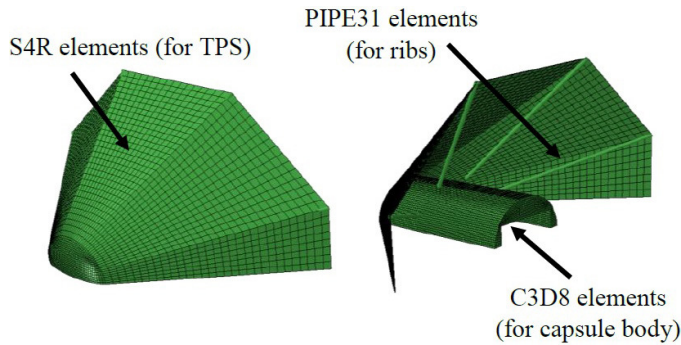


Figure 15: Capsule FEM

texture. This has been done in order to evaluate the TPS static deflection at the maximum stagnation point pressure condition along the flight re-entry trajectory based on the supersonic sounding rocket (REXUS) considered by Iacovazzo, Carandente, Savino and Zuppari (2015).

Figure 16 shows the results of the simulation. As can be seen, the maximum deflection is approximately 21.3 (mm).

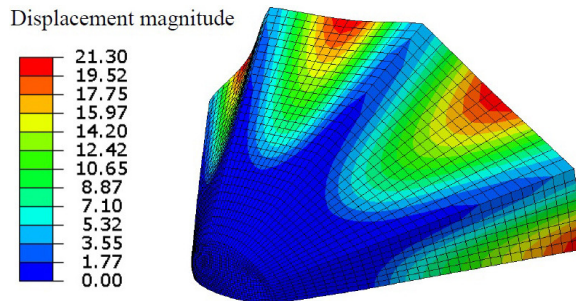


Figure 16: TPS deflection magnitude contour

Table 7: Capsule thermal materials properties

Material	Thickness (mm)	Density (Kg/m ³)	Conductivity (W/m·K)	Specific Heat (J/Kg·K)	Emissivity
Nextel 440-BF20	0.5	2700	0.15	1100	0.443
Aluminum Alloy 7075-T6	-	2700	237	880	0.1

4.3 Thermal Model

The heat transfer equations have been solved with *ABAQUS v6.13*. Due to symmetry conditions, only a quarter of the capsule has been modeled. Two materials have been selected, aluminum alloy 7075-T6 for the capsule body and Nextel 440-BF20 for the TPS (the properties of materials are in table 7). Numerical simulations have been performed in a three dimensional solid domain solving the energy equation with a coupled, time implicit numerical scheme.

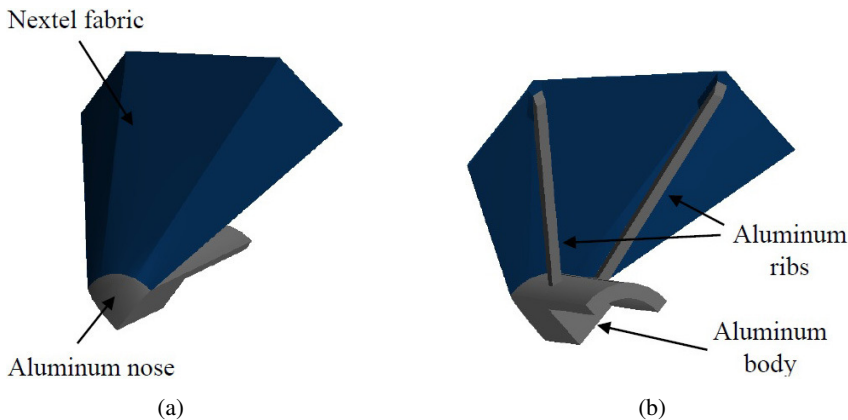


Figure 17: Capsule model front (a) and back (b)

A one-way approach has been considered, applying the constant convective heat flux distribution obtained by maximum heat flux condition CFD simulation illustrated in Section 4.1, in order to evaluate temperature distribution, without considering the iteration of the process. Therefore, a constant heat flux distribution of 6700 (W/m²) for the nose, and 2400 (W/m²) for the texture, have been applied on the front surface of the capsule. The radiative model takes into account the emissivity of the fabric (0.443) and of the aluminium (0.1) and an ambient temperature of 270 (K) is considered to simulate radiative heat transfer between the capsule and

the surrounding ambient. A four-layer fabric, made of Nextel 440-BF20, has been used for the TPS model. Temperature distribution results are shown in Figure 18 and 19.

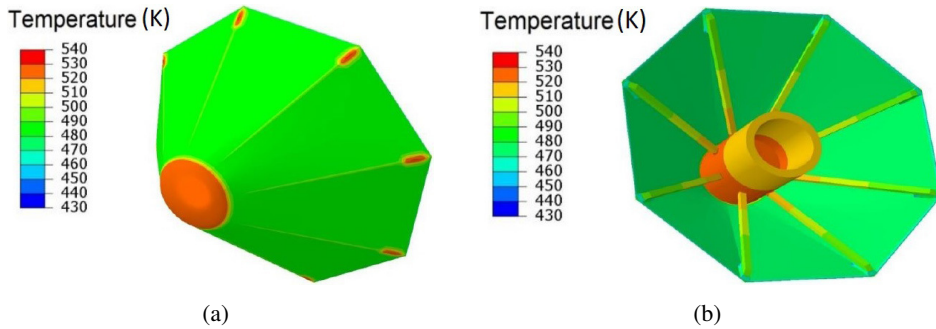


Figure 18: Temperature distribution front (a) and back (b)

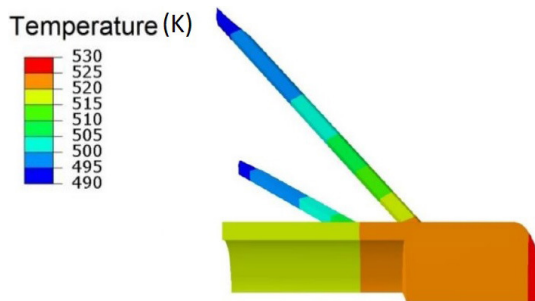


Figure 19: Capsule body temperature distribution

4.4 Capsule Aero-Thermal coupling

On the basis of the above considerations, an aero-thermal coupling using the partitioned approach presented in Section 3.2 has been performed. Only the maximum heat flux condition, reported in Table 1, has been simulated. In order to evaluate the thermal distribution inside the capsule body, it has been chosen to use the structural model illustrated in Section 4.3. As was done for the one-way approach, the radiation model that takes into account the emissivity of the fabric (0.443) and of the aluminum (0.1) and an ambient temperature of 270 (K) has been considered to simulate radiative heat transfer between the capsule and the surrounding ambient.

An implicit staggered numerical scheme (Figure 20) has been used to realize data transfer between the Fluid Dynamic solver *STAR-CCM+* and the FE structural

solver *ABAQUS*. In order to simulate a steady state condition a time step of 200 (s) and a maximum physical time of 60000 (s) have been set.

As shown in Figure 20, for each time step the boundary heat flux evaluated by the fluid solver is projected on the structural surface. Then, the FE solver calculates the temperature field and project it on the fluid domain. In an implicit time scheme, this transfer can occur more times per step, until convergence is reached.

Figures 21 and 22 show temperature distribution results in Kelvin.

Comparing Figures 18 and 21, the texture temperature remains nearly unchanged between the one-way approach and a two-way approach. This is due to the low thickness and the low conductivity of the material selected for the fabric. On the contrary, if we look at the temperature distribution of the capsule body (see Fig. 19 and 22), there is a slight difference in temperature profiles. This is due to the configuration and to the high conductivity of the aluminum (Table 7).

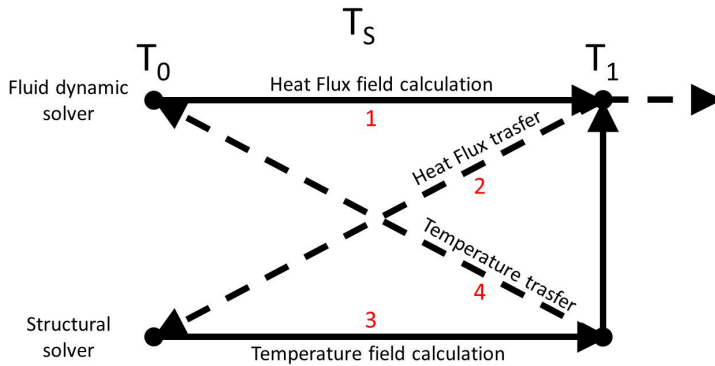


Figure 20: Implicit staggered algorithm for each time step

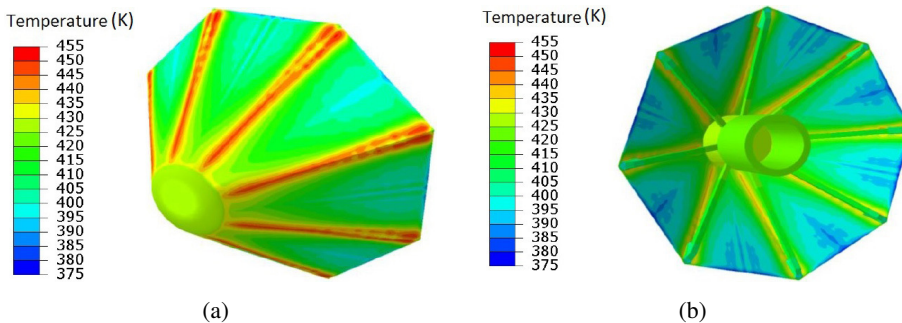


Figure 21: Temperature distribution front (a), and back (b)

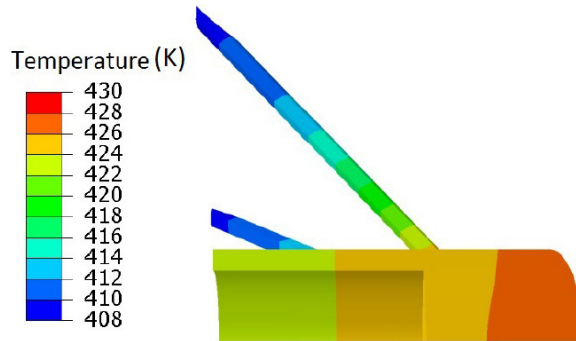


Figure 22: Capsule body temperature distribution

5 Concluding remarks

A relatively flexible partitioned approach using commercial codes has been analyzed to assess the aero-thermal behavior of Hypersonic Deployable re-entry systems. Preliminary evaluation of uncoupled structural, fluid dynamic and thermal behaviors have been obtained for a capsule configuration with a mechanically deployable TPS.

Thermo-structural comparisons have demonstrated the validity of ABAQUS code to evaluate deflections induced by temperature fields. A maximum percentage error of 10% has been calculated in the worst condition, comparing with the work of Gossard, for the case of a differential temperature of 339 (K).

Aero-thermal simulations have demonstrated the effectiveness of the partitioned approach presented in this work. As highlighted in Figure 11, despite same material properties and environmental conditions have been selected, results obtained using the CFD-FEM coupling approach presented in Section 3.2 are closer to experimental results obtained at NASA LaRC. This result permits to be more predictive in the design phase and provides the basis for a fully coupled CFD-FEM analysis, with the purpose to predict more accurately the Aero-Thermo-Dynamic behavior.

The aero-thermal analysis performed in this work on an HDAD, considering a typical suborbital reentry trajectory based on sounding rocket, illustrates the difference between a common one-way approach, and a two-way closely coupled partitioned approach.

As expected, this difference results particularly marked if we consider the thermal diffusion in a thick body with high conductivity. In this case, the possibility of using a Two-way approach, which takes into account the variation of the flow field due to the new thermal distribution inside the material, is more predictive in an

advanced design phase.

Moreover, we have calculated a maximum temperature of 428 (K) for the nose of the capsule and 455 (K) for the TPS fabric, which are significantly below nominal maximum temperatures that aluminum and Nextel could tolerate, allowing use of off-the-shelves materials for a typical suborbital re-entry trajectory based on a sounding rocket launch mission.

References

- Akin, D. L.** (1990): The parashield entry vehicle concept: basic theory and flight-test developments, in: *Proceedings of the 4th Annual AIAA/Utah State University Conference on Small Satellites*, Logan, UT, August 27–30.
- Bassano, E.; Savino, R.; Lo Forti, R.; Ferrarotti, A.; Richiello, C.; Russo, G.; Aurigemma, R.; Punzo, F.; Dell’Aversana, P.** (2011): IRENE – Italian re-entry nacelle for microgravity experiments, in: *Proceedings of the 62nd International Astronautical Congress*, CapeTown, October 3–7, IAC-11.A2.7.7.
- Beck, R. A. S.; Arnold, J. O.; White, S.; Fan, W.; Stackpoole, M.; Agrawal, P.; Coughlin, S.** (2011): Overview of initial development of flexible ablators for hypersonic inflatable aerodynamic decelerators, *21st AIAA Aerodynamic Decelerator Systems Technology Conference and Seminar 2011*.
- Bisplinghoff, R. L.; Dugundji, J.** (1958): Influence of Aerodynamic Heating on Aeroelastic Phenomena. Pergamon Press, 1958, pp. 288–312.
- Carandente, V.; Elia, G.; Savino, R.** (2013): Conceptual design of de-orbit and re-entry modules for standard CubeSats, in: *Proceedings of the 2nd IAA Conference on University Satellite Missions and Cubesat Work-shop*, Rome, February 4–7.
- Carandente, V.; Savino, R.** (2014): New concepts of deployable de-orbit and re-entry systems for CubeSat miniaturized satellites. *Recent Pat. Eng.*, vol. 8, pp. 2–12.
- Carandente, V.; Savino, R.; D’Orlando, V.; Fortezza, R.** (2014): Deployable aerobraking earth entry systems for recoverable microgravity experiments, in: *Proceedings of the 65th International Astronautical Congress, Toronto, Canada*, September 2014, IAC-14.A2.3.8.
- Carandente, V.; Savino, R.; Iacovazzo, M.; Boffa, C.** (2013): Aerothermal analysis of a sample-return reentry capsule. *Fluid Dynamics and Materials Processing*, vol. 9, no. 4, pp. 461–484.
- Carandente, V.; Zuppari, G.; Savino, R.** (2014): Aerothermodynamic and stability analyses of a deployable re-entry capsule. *Acta Astronautica*, vol. 93, pp. 291–303.

Cassell, A. M.; Swanson, G. T.; Keith Johnson, R.; Hughes, S. J.; Cheatwood, F. M. (2011): Overview of the hypersonic inflatable aerodynamic decelerator large article ground test campaign. *21st AIAA Aerodynamic Decelerator Systems Technology Conference and Seminar 2011*.

Culler, A. J.; McNamara, J. J. (2010): Studies on fluid-thermal-structural coupling for aerothermoelasticity in hypersonic flow. *AIAA Journal*, vol. 48, no. 8, pp. 1721–1738.

Del Corso, J. A.; Bruce, W. E.; Liles, K. A.; Hughes, S. J. (2011): Thermal Analysis and Testing of Candidate Materials for PAIDAE Inflatable Aeroshell. *21st AIAA Aerodynamic Decelerator Systems Conference*, Dublin, Ireland May 23–26.

Del Corso, J. A.; Cheatwood, F. M.; Bruce, W.; Hughes, S. J.; Calomino, A. M. (2011): Advanced high-temperature flexible TPS for inflatable aerodynamic decelerators. *21st AIAA Aerodynamic Decelerator Systems Technology Conference and Seminar*, AIAA Paper 2011–2510.

Deveikis, W. D.; Hunt, L. R. (1973): Loading and Heating of a Large Flat plate at mach 7 in the Langley 8-foot high-temperature structures tunnel. NASA-TN-D-7275, L-8760.

Glass, C. E.; Hunt, L. R. (1988): Aerothermal tests of quilted dome models on a flat plate at a mach number of 6.5. NASA-TP-2804, L-16346, NAS 1.60:2804.

Goldman, B. D.; Scott, R. C.; Dowell, E. H. (2014): Nonlinear Aeroelastic Analysis of the HIAD TPS Coupon in the NASA 8' High Temperature Tunnel: Theory and Experiment. NASA TM-2014-218267.

Goldman, B. D.; Dowell, E. H. (2015): In-Flight Aeroelastic Stability of the Thermal Protection System on the NASA HIAD, Part II Nonlinear Theory and Extended Aerodynamics. 56th AIAA/ASCE/AHS/ASC Structures, Structural Dynamics, and Materials Conference.

Goldman, B. D.; Dowell, E. H.; Scott, R. C. (2015): Aeroelastic stability of thermal protection system for inflatable aerodynamic decelerator. *Journal of Spacecraft and Rockets*, vol. 52, no. 1, pp. 144–156.

Gossard, M. L.; Seide, P.; Roberts, W. M. (1952): Thermal buckling of plates. NACA TN-2771.

Harper, B. P.; Braun, R. D. (2014): Preliminary Design Study of Asymmetric Hypersonic Inflatable Aerodynamic Decelerators for Mars Entry. AE8900 MS Special Problems Report, Guggenheim School of Aerospace Engineering Georgia Institute of Technology Atlanta, GA.

Hughes, S. J.; Cheatwood, F. M.; Dillman, R. A.; Wright, H. S.; Del Corso, J. A.; Calomino, A. M. (2011): Hypersonic Inflatable Aerodynamic Decelerator

(HIAD) technology development overview. *21st AIAA Aerodynamic Decelerator Systems Technology Conference and Seminar 2011*.

Hughes, S. J.; Dillman, R. A.; Starr, B. R.; Stephan, R. A.; Lindell, M. C.; Player, C. J.; Cheatwood, F. M. (2005): Inflatable Re-entry Vehicle Experiment (IRVE) Design Overview. 18th AIAA Aerodynamic Decelerator Systems Technology Conference and Seminar, Munich, Germany, May 24–26.

Hughes, S. J.; Ware, J. S.; Del Corso, J. A.; Lugo, R. A. (2009): Deployable aeroshell flexible thermal protection system testing. *20th AIAA Aerodynamic Decelerator Systems Conference*.

Iacovazzo, M.; Carandente, V.; Savino, R.; Zuppari, G. (2015): Longitudinal stability analysis of a suborbital re-entry demonstrator for a deployable capsule. *Acta Astronautica*, vol. 106, pp. 101–110.

Kramer, R. M. J.; Cirak, F.; Pantano, C. (2013): Fluid–structure interaction simulations of a tension-cone inflatable aerodynamic decelerator. *AIAA Journal*, vol. 51, no. 7, pp. 1640–1656.

Litton, D. K.; Bose, D. M.; Cheatwood, F. M.; Hughes, S.; Wright, H. S.; Lindell, M. C.; Derry, S. D.; Olds, A. (2011): Inflatable re-entry vehicle experiment (IRVE) - 4 overview. *21st AIAA Aerodynamic Decelerator Systems Technology Conference and Seminar 2011*.

McNamara, J. J.; Friedmann, P. P. (2007): Aeroelastic and aerothermoelastic analysis of Hypersonic vehicles: Current status and future trends. *Collection of Technical Papers - AIAA/ASME/ASCE/AHS/ASC Structures, Structural Dynamics and Materials Conference*, pp. 3814.

McNamara, J. J.; Friedmann, P. P. (2011): Aeroelastic and aerothermoelastic analysis in hypersonic flows: past, present, and future. *AIAA Journal* vol. 49, no. 6, pp. 1089–1122.

Savino, R.; Aurigemma, R.; Carandente, V.; Dell'Aversana, P.; Gramiccia, L.; Longo, J.; Marraffa, L.; Punzo, F. (2013): Study and development of a sub-orbital reentry demonstrator, in: Proceedings of the Italian Association of Aeronautics and Astronautics XXII Conference, Naples, Italy, September 9–12.

Savino, R.; Carandente, V. (2012): Aerothermodynamic and feasibility study of a deployable aero-braking re-entry capsule, *Fluid Dyn. Mater. Process*, vol. 8, no. 4, pp. 453–477.

Sheta, E. F.; Venugopalan, V.; Tan, X. G.; Liever, P. A.; Habchi, S. D. (2010): Aero-structural assessment of an inflatable Aerodynamic Decelerator. NASA/CR-2010-216731, CFDRC Rept-8927/6, NF1676L-10953.

Smith, B. P.; Tanner, C. L.; Mahzari, M.; Clark, I. G.; Braun, R. D.; Cheatwood, F. M. (2010): A historical review of inflatable aerodynamic decelerator technology development, *IEEE Aerospace Conference Proceedings*.

Wang, Z.; Yang, S.; Liu, D. D.; Wang, X. Q.; Mignolet, M. P.; Bartels, R. E. (2010): Nonlinear aeroelastic analysis for a wrinkling aeroshell/ballute system. *Collection of Technical Papers - AIAA/ASME/ASCE/AHS/ASC Structures, Structural Dynamics and Materials Conference*.

Wilde, D.; Walther, S. (2001): Inflatable Re-entry and Descent Technology (IRDT)—further developments, in: *Proceedings of the 2nd International Symposium of Atmospheric Re-entry Vehicles and Systems*, Arcachon, France.